

# Electronic structure of single-crystalline $\text{Mg}_x\text{Al}_{1-x}\text{B}_2$

S. Schuppler,<sup>1</sup> E. Pellegrin,<sup>1</sup> N. Nücker,<sup>1</sup> T. Mizokawa,<sup>2</sup> M. Merz,<sup>3</sup> D. A. Arena,<sup>4</sup> J. Dvorak,<sup>5</sup> Y. U. Idzerda,<sup>5</sup> D.-J. Huang,<sup>6</sup> C.-F. Cheng,<sup>6</sup> K.-P. Bohnen,<sup>1</sup> R. Heid,<sup>1</sup> P. Schweiss,<sup>1</sup> and Th. Wolf<sup>1</sup>

<sup>1</sup> *Forschungszentrum Karlsruhe, Institut für Festkörperphysik, D-76021 Karlsruhe, Germany*

<sup>2</sup> *Department of Complexity Science and Engineering, University of Tokyo, Tokyo 113-0033, Japan*

<sup>3</sup> *Institut für Kristallographie, Rheinisch-Westfälische Technische Hochschule Aachen, D-52056 Aachen, Germany*

<sup>4</sup> *Naval Research Laboratory, Code 6345, Washington DC 20365, USA*

<sup>5</sup> *Department of Physics, Montana State University, Bozeman, MT 59717, USA*

<sup>6</sup> *Synchrotron Radiation Research Center, No. 1 R&D Road VI, Hsinchu 30077, Taiwan*

(Received May 10, 2002)

Polarization-dependent x-ray absorption spectroscopy at the B 1s edge of single-crystalline  $\text{Mg}_x\text{Al}_{1-x}\text{B}_2$  reveals a strongly anisotropic electronic structure near the Fermi energy. Comparing spectra for superconducting compounds ( $x=0.9, 1.0$ ) with those for the non-superconductor  $x=0.0$  gives direct evidence on the importance of an in-plane spectral feature crossing  $E_F$  for the superconducting properties of the diborides. Good agreement is found with the projected B 2p density of states from LDA band structure calculations.

$\text{MgB}_2$  is a compound known for decades which only recently, to everyone's surprise, was shown to be a superconductor [1] with  $T_c \approx 39$  K, one of the highest transition temperatures observed for any non-cuprate material. Compared to the high- $T_c$  cuprates its crystal structure is simple: boron and magnesium form separate layers ("in-plane" lattice constant  $a \approx 3.09$  Å) which, for B, are graphite-like with a hexagonal atomic arrangement. The B and Mg sheets are stacked alternately along the  $c$  axis ("out-of-plane" lattice constant  $c \approx 3.52$  Å). This layered structure, and especially the covalent  $sp^2$  and 2D character of the B-B  $\sigma$  bonds [2], already suggests a strong anisotropy between in-plane and out-of-plane properties [3]. It was established quickly [4,5] by experiment and theory that superconductivity in this compound is fairly conventional, being  $s$ -wave, BCS-type, and phonon-induced. Recently, however, also deviations were suggested, like the presence of two energy gap scales [6]. Substitution of Mg by Al is, at high temperatures, possible for all concentrations, preserving the crystal structure while decreasing lattice constants (slightly in the case of  $a$ , considerably in the case of  $c$  [7]); electron doping, combined with increased orbital overlap due to unit volume contraction, is expected during this substitution, and superconductivity is very quickly suppressed at only modest substitution levels [8].

The electronic structure near the Fermi level,  $E_F$ , has been studied by photoemission, x-ray absorption, and optical experiments, first on polycrystalline samples [9,10,11,12], and now augmented by de Haas-van Alphen investigations [13]. Single crystals which recently became available [14] allow studies in even greater depth, like determining occupied band dispersions in angle-resolved photoemission [15]. More immediate access to the *orbital* character is provided by polarization-dependent near-edge x-ray absorption fine structure (NEXAFS) experiments; we present the first such study on single-

crystalline  $\text{Mg}_x\text{Al}_{1-x}\text{B}_2$ , which, performed at the boron 1s edge, yields the unoccupied electronic structure with B 2p character (as a function of Al substitution) and is able to discriminate between  $\sigma$  and  $\pi$  states. Spectral results are directly compared with the appropriately projected B 2p density of electronic states (DOS) from LDA band structure calculations, enabling us to sensitively test and possibly cross-corroborate the theoretical and experimental electronic structure near  $E_F$ .

Single crystals of  $\text{AlB}_2$  and the solid solution  $\text{Mg}_{0.9}\text{Al}_{0.1}\text{B}_2$  were grown from Al or Al/Mg flux by the slow-cooling method; the resulting crystal sizes were about  $2 \times 2$  mm<sup>2</sup> for  $x=0$  and  $0.4 \times 0.5$  mm<sup>2</sup> for  $x=0.9$ . Hexagonal single-crystalline  $\text{MgB}_2$  platelets with a diameter of up to 200  $\mu\text{m}$  could be obtained by isothermally annealing <sup>11</sup>B powder [16] in a Mg flux enclosed in an evacuated Mo cylinder. The  $\text{MgB}_2$  crystals ( $x=1$ ) show a sharp superconducting transition at  $T_c=38.8$  K, with a resistive 10%-90% width  $\Delta T \approx 1.8$  K. The substitution level,  $x=0.9$ , of the partially Al substituted crystals was determined by x-ray diffraction; the transition was already suppressed to around 20 K and considerably broadened. To increase useful surface area for  $x=0.9$  and 1.0, several crystals were mounted right next to each other on the sample holder [17].

Near-edge x-ray absorption fine structure (NEXAFS) measurements with linearly polarized light were performed at two facilities: the National Synchrotron Light Source (NSLS), Brookhaven, USA, where the Montana State University/NSLS beamline U4B was utilized for measuring the  $x=0$  sample; and at the Synchrotron Radiation Research Center (SRRC), Hsinchu, Taiwan, where the undulator beamline U5 was used for measuring the  $x=0.9$  and  $x=1.0$  samples. Resolution was set to 180 and 100 meV at the NSLS and the SRRC, resp.; all data were taken in the normal state. Cleaving the samples was obviated by employing bulk-sensitive fluorescence-yield (FY)

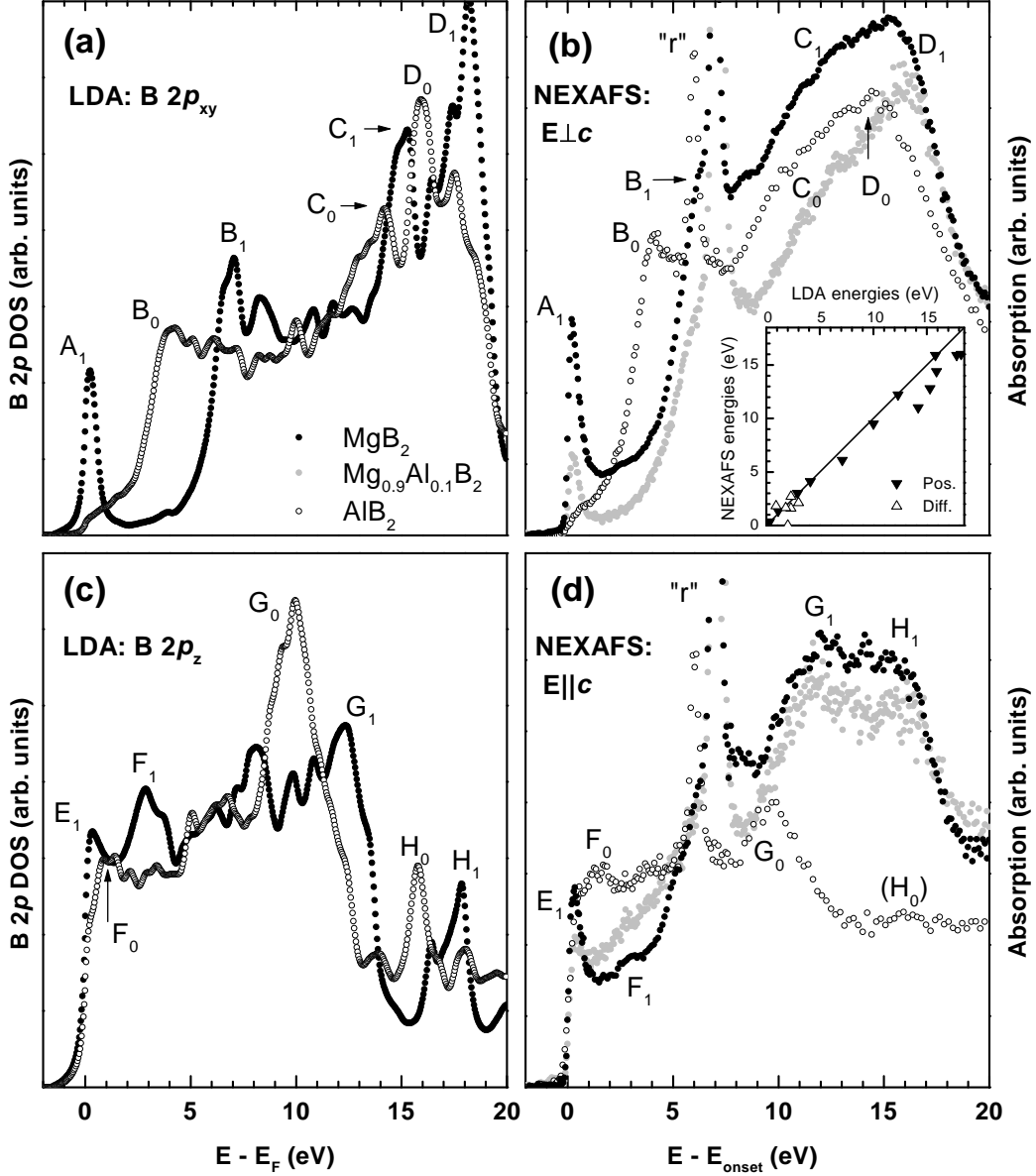


FIG. 1. Orbital-specific electronic structure of single-crystalline  $MgB_2$  (black circles),  $Mg_{0.9}Al_{0.1}B_2$  (grey circles), and  $AlB_2$  (open circles): (a) Projected unoccupied density of states (DOS) with B  $2p_{xy}$  (“in-plane”) character from LDA band structure calculations. (b) B  $1s$  near-edge x-ray absorption (fluorescence yield detection) with the polarization of the incident radiation,  $\mathbf{E}$ , oriented parallel to the base planes, probing the unoccupied B  $2p_{xy}$  density of states. (c) As (a), but showing the theoretical unoccupied DOS with B  $2p_z$  (“out-of-plane”) character. (d) As (b), but with  $\mathbf{E} \parallel c$ , probing the unoccupied B  $2p_z$  density of states. Inset: Comparison NEXAFS *vs.* LDA. Full symbols denote peak positions; good correspondence to the NEXAFS=LDA line indicates that correlation effects are small. Open symbols denote the energy shifts between  $AlB_2$  and  $MgB_2$  for all major peak pairs  $X_0/X_1$  ( $X=B \dots H$ ); the clustering around 2 eV points to a “semi-rigid” band shift by that value.

detection with a typical probing depth of  $\approx 500$  Å, using either a channeltron (SRRC) or Si(Li) detectors (NSLS). The necessary self-absorption correction was performed [18] using tabulated cross sections [19]. While the energy-dispersive Si(Li) detectors allowed direct suppression of the mainly Mg/Al  $2p$ -derived and energy-dependent background, this background had to be numerically removed (using the same tables) for the channeltron spectra. Some residual distortion remains, and spectral

weights for the latter, i. e., for  $MgB_2$  and  $Mg_{0.9}Al_{0.1}B_2$ , cannot quantitatively be compared to those for  $AlB_2$ . Spectra were taken at normal incidence (polarization parallel to the crystal base plane, i. e.,  $\mathbf{E} \perp c$ ) and at  $60^\circ$  grazing incidence; the  $\mathbf{E} \parallel c$  spectra were extrapolated. Energy calibration is approximated by extrapolation from the O  $1s$  edge of a reference system and yields a  $MgB_2$  onset position near 186 eV.

LDA band structure calculations up to 20 eV above the

Fermi level  $E_F$  were performed in the mixed-basis pseudopotential framework [20], with 18/18/18 Monkhorst-Pack  $k$  sampling in the Brillouin zone (BZ) and using the tetraeder method for determining the electronic density of states (DOS); further details can be found in Ref. [5]. The occupied states (which are not observable in x-ray absorption) were separated off, and convolution with a Gaussian of width 0.2 eV roughly simulates experimental broadening effects, including core-hole lifetime, multiphonon processes, and monochromator resolution. In the absence of strong correlation and/or excitonic effects the resulting B  $2p$  DOS should closely resemble the experimental spectra.

Figure 1 presents the main results of this work. It is divided into four panels (a)–(d): the left column [(a), (c)] contains the theoretical results and the right column [(b), (d)] the experimental ones; the upper row [(a), (b)] plots the in-plane spectra, the lower row [(c), (d)] the out-of-plane spectra. Data for  $x=1.0$  (MgB<sub>2</sub>) are depicted as black circles in all panels, those for  $x=0.9$  as grey circles, and those for  $x=0$  (AlB<sub>2</sub>) as open circles. To facilitate further discussion the main features in the spectra are labeled A...H, with subscripts “1” and “0” denoting features corresponding to samples with or without Mg. A number of observations immediately catches the eye and is discussed in the following:

(i) Most obvious is the strong asymmetry between in-plane and out-of-plane spectra, illustrating the different character of B  $2p$   $\sigma$  and B  $2p$   $\pi$  states, resp., and also underlining the need for such a polarization- and thus symmetry-resolved study.

(ii) In NEXAFS (but not in LDA), a sharp spike is observed around 6–7 eV above onset for both orientations (and for  $x=1.0$  and 0.9 extending above the intensity region shown). It is attributed to one of the resonances identified in Ref. [10] (and is thus labeled “r” in our Figure 1) [21]. This feature does not affect the electronic structure near onset and can thus be disregarded in the following.

(iii) The general agreement between theory and experiment is, on all accounts, excellent: all major spectral features are reproduced nicely, not only in their energy positions (Table I provides a listing) but often also in their relative spectral weight. For the *in-plane* spectra of MgB<sub>2</sub> the LDA results (Fig. 1 (a)) show right above  $E_F$  a prominent peak A<sub>1</sub> derived from a region of low dispersion along the A line in the BZ (the uppermost part of the almost fully occupied, bonding  $\sigma$  band derived from B  $2p_{xy}$  states). This is followed by a region of very low (but non-zero) DOS until a steep rise up to a shoulder B<sub>1</sub> occurs about 7 eV above  $E_F$ ; between 14 and 20 eV a large maximum D<sub>1</sub> is preceded by a shoulder C<sub>1</sub> and followed by a steep decrease to low DOS. NEXAFS data (Fig. 1 (b)) display the same feature A<sub>1</sub> right at onset, very prominently and sharp. In fact, the width of this feature, 0.7 eV, is exactly the theoretical value. Although

the spectral intensity right above A<sub>1</sub> is, in agreement with theory, substantially reduced the suppression is not quite as complete since the NEXAFS experiment does not exactly image the DOS but starts developing an absorption jump. B<sub>1</sub> is partially masked by the oxide-related peak “ox”, but peak D<sub>1</sub> (with shoulder C<sub>1</sub> before and steep decrease afterwards) reproduces again nicely the averaged LDA structure in this energy range. The in-plane spectra of AlB<sub>2</sub> exhibit for both LDA and NEXAFS a very low DOS for about 2 eV above  $E_F$  and onset, resp. – there is no peak A<sub>0</sub> visible, suggesting that this feature (which would correspond to A<sub>1</sub>) is already occupied and situated below  $E_F$ . Only after several eV the spectra rise to a shoulder with small protrusion B<sub>0</sub> at about 4 eV above  $E_F$ . D<sub>0</sub>, again with preceding shoulder C<sub>0</sub> and subsequent fall-off, is somewhat less pronounced compared to the similar feature for MgB<sub>2</sub>.

While NEXAFS for Mg<sub>0.9</sub>Al<sub>0.1</sub>B<sub>2</sub> in general resembles that for MgB<sub>2</sub> quite closely it is conspicuous that even at this small substitution level peak A<sub>1</sub> has already lost much of its spectral weight, about 65% compared to MgB<sub>2</sub>. Close inspection also indicates an A<sub>1</sub> width reduced by about 0.1 eV (less than all experimental broadening; the intrinsic width reduction will thus be greater). With this, and assuming that the Al content injects 0.1 electrons per formula unit, one can crudely estimate the B  $2p_x$  DOS at  $E_F$  to be  $\lesssim 0.37$  states/(eV·atom); LDA estimates 0.10 states/(eV·atom). Obviously small additional substitution will push A<sub>1</sub> below  $E_F$  altogether, consistent with the quick suppression of superconductivity reported for Al doping.

(iv) For the *out-of-plane* orientation LDA (Fig. 1 (c)) predicts, in contrast to the in-plane spectra, an almost constant DOS for about 5 eV above  $E_F$  for both MgB<sub>2</sub> and AlB<sub>2</sub>. Although the corresponding  $\pi$  bonds give less rise to dramatic DOS variations than the  $\sigma$  bonds discussed in (iii) some more features can be identified and exhibit, again, good correspondence between theory and experiment. Differences worth noting are very few: peak H<sub>0</sub> is almost undetectable in experiment while H<sub>1</sub> is stronger in weight than in LDA; both are, on the other hand, located 15 eV and more above  $E_F$  where precise correspondence between x-ray absorption and band structure is less to be expected. Right at  $E_F$ , however, peak E<sub>1</sub> for MgB<sub>2</sub> appears considerably stronger in NEXAFS than in LDA; imperfections in mounting the small crystallites may have introduced some angular uncertainty which could cause some contribution from in-plane A<sub>1</sub> intensity.

The inset in Fig. 1 (b) further illustrates the good agreement between LDA and NEXAFS: the peak positions (full symbols) lie, up to 12 eV and more, very close to the straight line denoting exact, 1:1 correspondence; the tendency visible at higher energies towards reduced NEXAFS energies does not suggest a significant amount of correlation. The open symbols depict the corresponden-

	$E  a$			$E  c$	
	LDA	NEXAFS		LDA	NEXAFS
A <sub>1</sub>	0.2	0.2	E <sub>1</sub>	0.3	0.3
B <sub>0</sub>	4.1	4.1	F <sub>0</sub>	1.1	1.3
B <sub>1</sub>	7.1	6.1	F <sub>1</sub>	2.9	3.0
"r" <sub>0</sub>	–	6.0	"r" <sub>0</sub>	–	6.0
"r" <sub>1</sub>	–	7.0	"r" <sub>1</sub>	–	7.0
C <sub>0</sub>	14.2	≈11	G <sub>0</sub>	10.0	9.5
C <sub>1</sub>	15.3	≈13	G <sub>1</sub>	12.3	12.2
D <sub>0</sub>	15.9	14.3	H <sub>0</sub>	15.8	(≈16)
D <sub>1</sub>	18.2	≈16	H <sub>1</sub>	17.8	15.9

Table 1: Energy positions of the major spectral features in B 1s NEXAFS measurements compared to those in the B 2p density of states from LDA band structure calculations. All energies  $E$  are given in eV, and are referred to the Fermi level  $E_F$  (LDA) and spectral onset (NEXAFS). A subscript "1" at each peak label denotes features of  $\text{Mg}_1\text{Al}_0\text{B}_2$  or  $\text{Mg}_{0.9}\text{Al}_{0.1}\text{B}_2$ , a subscript "0" denotes those for  $\text{Mg}_0\text{Al}_1\text{B}_2$ .

ces between the peak pairs for  $\text{AlB}_2$  and  $\text{MgB}_2$ , like  $B_0/B_1$ , many of which are to some degree consistent with a "semi-rigid shift" of the band structure [2] due to the extra electron per formula unit introduced by Al replacing Mg. The symbols cluster around a value of 2 eV for such a shift.

In conclusion, the orbital-resolved electronic structure of the novel superconductor  $\text{MgB}_2$  was studied with polarization-dependent B 1s NEXAFS on single crystals and was compared to NEXAFS on single-crystalline  $\text{Mg}_{0.9}\text{Al}_{0.1}\text{B}_2$  and non-superconducting  $\text{AlB}_2$  as well as to the unoccupied B 2p DOS obtained from LDA band structure for both  $\text{MgB}_2$  and  $\text{AlB}_2$ . The similarity between LDA and NEXAFS is excellent for a large number of major spectral features – in particular, a B 2p<sub>xy</sub>  $\sigma$  derived state at  $E_F$  that is identified by theory to carry superconductivity shows up very prominently in  $\text{MgB}_2$  NEXAFS, is already considerably reduced for  $\text{Mg}_{0.9}\text{Al}_{0.1}\text{B}_2$ , and is completely absent (i. e., occupied) for  $\text{AlB}_2$ . Less drastic changes are observed for the B 2p<sub>z</sub>  $\pi$  states. Systematics in peak positions are consistent with a semi-rigid shift of the bands expected from the extra electrons provided by Al. The close correspondence between experiment and theory lends additional and valuable support to further theoretical implications, including the absence of strong correlation effects, the dominant effect of holes in the B 2p  $\sigma$  bands (as compared to the  $\pi$  bands) for superconductivity, as well as its BCS-type mechanism and electron-phonon origin, in this family of layered, covalent compounds.

We thank C. T. Chen, S.-C. Chung, S. L. Hulbert, H.-J. Lin, G. Nintzel, S. Tokumitsu, and H. Winter for generous support and fruitful discussions. This work was supported by the German Academic Exchange Service (DAAD) and the National Science Council, Taiwan (NSC). Research was carried out in part at the NSLS, Brookhaven National Laboratory, which is supported by the U. S. Department of Energy, Division of Material Sci-

ences and Division of Chemical Sciences, under contract number DE-AC02-98CH10886.

- 
- [1] J. Nagamatsu *et al.*, Nature **410**, 63 (2001).
  - [2] J. M. An and W. E. Pickett, Phys. Rev. Lett. **86**, 4366 (2001).
  - [3] The silvery-golden hue of the cleavage planes in contrast to the purely golden hue of the side faces visualizes an anisotropy in plasmon energies and electron densities.
  - [4] See, e. g., S. L. Bud'ko *et al.*, Phys. Rev. Lett. **86**, 1877 (2001); G. Rubio-Bollinger *et al.*, Phys. Rev. Lett. **86**, 5582 (2001).
  - [5] K.-P. Bohnen, R. Heid, and B. Renker, Phys. Rev. Lett. **86**, 5771 (2001); B. Renker *et al.*, Phys. Rev. Lett. **88**, 067001 (2002).
  - [6] A. Y. Liu, I. I. Mazin, and J. Kortus, Phys. Rev. Lett. **87**, 087005 (2001); X. K. Chen *et al.*, Phys. Rev. Lett. **87**, 157002 (2001).
  - [7] O. de la Pena, A. Aguayo, and R. de Coss, cond-mat/0203003 (2002).
  - [8] J. S. Slusky *et al.*, Nature **410**, 343 (2001).
  - [9] T. Takahashi *et al.*, Phys. Rev. Lett. **86**, 4915 (2001).
  - [10] T. A. Callcott *et al.*, Phys. Rev. B **64**, 132504 (2001).
  - [11] J. Nakamura *et al.*, Phys. Rev. B **64**, 174504 (2001).
  - [12] B. Gorshunov *et al.*, Eur. Phys. J. B **21**, 159 (2001).
  - [13] H. Rosner *et al.*, cond-mat/0203030 (2002); I. I. Mazin and J. Kortus, cond-mat/0201247 (2002).
  - [14] S. Lee *et al.*, J. Phys. Soc. Jpn. **70**, 2255 (2001).
  - [15] H. Uchiyama *et al.*, Phys. Rev. Lett. **88**, 157002 (2002).
  - [16] Pure  $^{11}\text{B}$  was used to facilitate neutron scattering.
  - [17] In-plane orientation is irrelevant due to the hexagonal symmetry.
  - [18] S. Gerhold *et al.*, Phys. Rev. B (submitted).
  - [19] J. J. Yeh and I. Lindau, At. Data Nucl. Data Tab. **32**, 1 (1985).
  - [20] B. Meyer, C. Elsässer, and M. Fähnle, "FORTRAN90 Program for Mixed-Basis Pseudopotential Calculations for Crystals," Max-Planck-Institut für Metallforschung, Stuttgart (unpublished).
  - [21] Probably the resonance peak is oxide-related (*cf.* peak C in Ref. [10]), although we cannot exclude an origin in resonant elastic scattering [10]. Assuming the former, our own self-absorption corrected FY-NEXAFS amplitudes, when compared to the amplitudes recorded simultaneously with surface-sensitive total electron yield detection, do not support the conjecture [10] that the oxide be located in a surface region. The resonant enhancement, on the other hand, means that the oxide content is likely to be small. Moreover, the "white line" in the oxide NEXAFS is the lowest-lying spectral feature there, so no oxide contribution will appear in our  $\text{Mg}_x\text{Al}_{1-x}\text{B}_2$  spectra down to the onset.